Prompt fission neutrons from eV resonances in ^{235}U: Measurement and correlation with other fission properties*

R. E. Howe and T. W. Phillips
Lawrence Livermore Laboratory, University of California, Livermore, California 94550

C. D. Bowman
National Bureau of Standards, U.S. Department of Commerce, Washington, D.C. 20234

(Received 28 July 1975)

The energy dependence of the fission neutron multiplicity $\bar{\nu}$ for neutron-induced fission of ^{235}U in the energy region 0.5 to 125 eV has been measured using a continuous spectrum of neutrons from a 100 MeV electron Linac. A new neutron detection technique was used to search for variations in resonance $\bar{\nu}$ values and possible correlations with other fission properties. Evidence was obtained for a nonstatistical fluctuation in the value of $\bar{\nu}$ as a function of energy. However, no correlation with resonant spin, Γ_f, fission-fragment asymmetry, or the angular distribution of fission fragments was observed. A comparison of these data with previous $\bar{\nu}$ measurements also has been included.

[RADIOACTIVITY fission ^{235}U (n,f), $E=0.5$–125 eV; measured relative $\bar{\nu}_n$, deduced correlations with other fission properties.]

INTRODUCTION

The variation of $\bar{\nu}$ (the average number of prompt fission neutrons) from resonance to resonance has remained an open question both theoretically and experimentally. Previous measurements have found distributions of $\bar{\nu}$ values which appeared to cluster about two means.[1-4] This observation led to the suggestion that $\bar{\nu}$ is correlated with the spin of the resonance which for low energy neutron-induced fission is restricted to two values ($J \pm \frac{1}{2}$, where J is the spin of the target nucleus). Further speculation regarding which spin would have the larger multiplicity has been made on the basis of both experimental evidence and theoretical ideas. It has been observed that more neutrons are emitted for fission leaving fragments of equal mass than for asymmetric division.[5] Experiments have been performed which indicate that the spin ($J=3$) resonances of ^{235}U have lower yields of symmetric fission.[6] Thus $\bar{\nu}$ for resonances with spin 4^- should be greater than for 3^-. These experimental results are in agreement with simple theoretical considerations regarding the position of the fission barrier for the two spin states in ^{235}U. However, similar considerations for ^{239}Pu give predictions which appear to be contradictory to experiment. It has also been pointed out that the exit channel is critical in determining the properties of fission.[7] In the case of ^{235}U the spins of the resonances excited by low energy neutrons do not select a particular exit channel and therefore fission properties would not be expected to correlate with the spin of the resonances.[8]

The experimental evidence prior to this measurement for a variation of $\bar{\nu}$ from resonance to resonance was also contradictory. For the case of ^{235}U, Ryabov *et al.*[2] found a grouping of $\bar{\nu}$ about two mean values separated by about 2% for the resonance energy region: 1–40 eV; while Weinstein, Reed, and Block[1] found a separation of only 0.7%. Further, a resonance-by-resonance comparison of these measurements showed them to be nearly anticorrelated [large values of $\bar{\nu}$ in one measurement correlated with small values in the other (Fig. 1)]. Similar contradictory evidence was found for the case of ^{239}Pu.[1-3]

With the aim of resolving these conflicting experiments and theories, the energy dependence of $\bar{\nu}$ for ^{235}U (n,f) was measured by a new method. This method was designed to circumvent some of the problems of previous techniques. In subsequent sections this new technique, the analysis of the data it yielded, and the results of this analysis are discussed.

EXPERIMENT

In order to measure the variation of $\bar{\nu}$ with incident neutron energy, 100 mg of ^{235}U deposited on several foils in a fission ionization chamber was irradiated by the neutron beam from the LLL 100-MeV linear electron accelerator. The chamber was positioned inside the apparatus for detecting the prompt fission neutrons at the end of a 13.1-m flight path (see Fig. 2). The energies of the incident neutrons which produced fission events observed in the chamber were determined by measuring their flight times along this path. Prompt neutrons from the fission process were

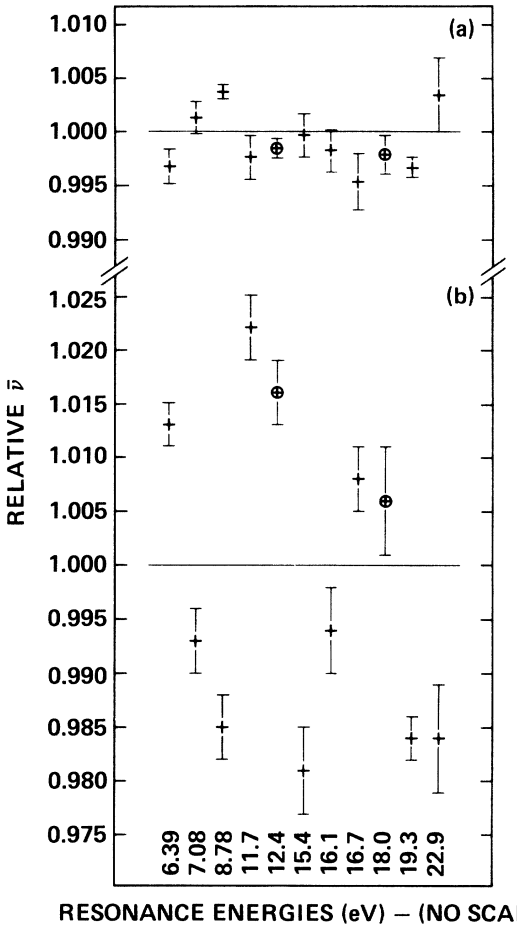

FIG. 1. Resonance data for ^{235}U prior to the design of the present experiment. Data in Fig. 1(a) are taken from Weinstein *et al.* (Ref. 1); those in Fig. 1(b) are from Ryabov *et al.* (Ref. 2). Both groups of data were individually renormalized to a weighted mean of 1. Plotted symbols denote the spin state assigned to a particular resonance and were taken from a measurement by Keyworth *et al.* (Ref. 9). The ⊕ is used for $J=3^-$; the + denotes resonances with $J=4^-$. Resonance energies are from Ref. 10. Note apparent discrepancies.

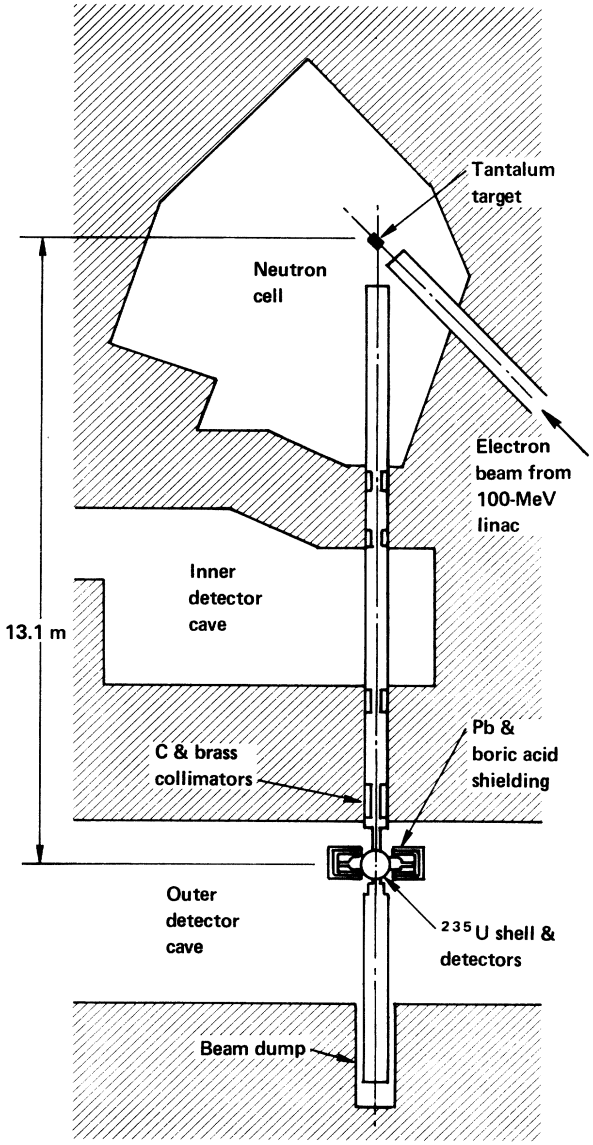

FIG. 2. Neutron time-of-flight arrangement for present experiment. Hatched areas represent concrete shielding.

identified by coincident signals in the fission chamber and the neutron detector. These events were sorted with respect to flight time by an on-line computer.

The aspect of the experimental procedure which departed most radically from previous measurements was the fission neutron detection system. An ideal neutron detector for a $\bar{\nu}$ measurement should respond only to the number of neutrons and be independent of their energy spectrum. However, if the energy spectrum of prompt fission neutrons were independent of incident neutron energy, any detector sensitive only to neutrons would be adequate. Short response time was an additional requirement placed on the neutron detection apparatus. The small duty factor of the linear accelerator and the desire to extend the $\bar{\nu}$ measurements to high energies led to this requirement.

Previous measurements of $\bar{\nu}$ employed two schemes for neutron detection. Three authors used large Gd- or Cd-loaded liquid scintillators,[1,2,4,11] and one[3] used proton-recoil scintillators separated from the fission source by 2.5 cm of lead to attenuate γ rays from fission and

short-lived products. The first of these methods is quite insensitive to changes in the fission neutron spectrum, since all neutrons are first moderated in the scintillator tank prior to capture in the Gd or Cd. However, these devices require long counting times (~30–50 μsec) during which the neutrons are moderated and captured. Neutron background and dead-time problems are enhanced by this long counting period. Sensitivity to delayed γ rays from the short-lived fission products increases the background problem. The short flight times involved with MeV incident neutron energies make high energy $\bar{\nu}$ measurements impossible when these relatively slow detectors are used with pulsed "white" neutron sources such as linacs.

The proton-recoil scintillators circumvent many of these difficulties owing to their relatively short response times (~25–250 nsec) and by the availability of pulse-shape discrimination (PSD) to separate neutrons and γ rays. However, the response function of these detectors drops sharply for neutron energies less than about 500 keV. Thus an important fraction of the fission neutron spectrum goes undetected and may lead to discrepancies in the value of $\bar{\nu}$ deduced from these measurements if the spectrum varies from resonance to resonance.

In order to cope with these problems, the detector system shown in Fig. 3 was developed. This detection system differs from others using proton-recoil detectors by the addition of a shell of ^{235}U enclosing the fission target. The prompt fission neutrons from the target under study interact with the ^{235}U shell and produce secondary fissions therein. These secondary neutrons are then detected via the proton-recoil scintillations produced in liquid benzene scintillators. Since the

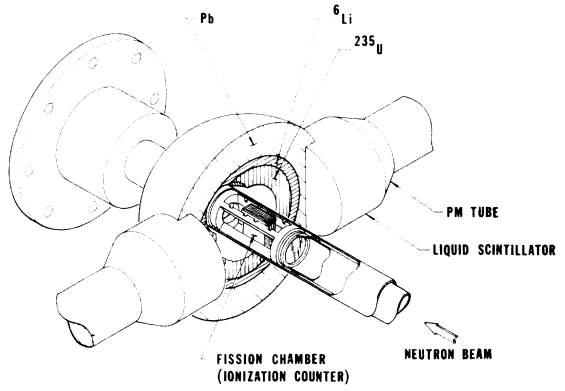

FIG. 3. Fission neutron detector for the present $\bar{\nu}$ measurement. The outer diameter of the lead spherical shell is ~300 mm. The fission chamber containing pipe is ~60 mm in diameter.

^{235}U fission cross section is slowly varying over the energy range of the fission spectrum the shell response to the prompt fission neutrons is nearly independent of their energy spectrum and proportional only to their number. $\bar{\nu}$ is then obtained as a function of incident neutron energy by comparing the number of fissions occurring to the number of fissions accompanied by a neutron in the proton-recoil scintillators.

The ^{6}Li shell is employed for several reasons. It shields the system from room background thermal neutrons which would produce fissions in the ^{235}U shell and would thereby raise the neutron background in the scintillators. The ^{6}Li also helps to make the system faster by reducing the effectiveness of slower neutrons in the multiplication process. By so doing it also aids in minimizing the fission-scintillation coincidence time interval which lowers the effectiveness of the background events that do exist.

The Pb shell is used to aid the multiplication process by reflecting many of the escaping keV and MeV neutrons (~60%). Together with the ^{235}U shell it also provides considerable high-Z material to attenuate the prompt fission γ rays from the ^{235}U target material (~120 : 1) and from secondary fissions in the ^{235}U shell (~35 : 1).

The 2.9-cm thick ^{235}U shell together with the surrounding shells of ^{6}Li and Pb manifest a criticality $k = 0.75$.[12] This provides an over-all neutron multiplication of 4.0. About 70% (or 2.81 per source neutron) of these neutrons ultimately leave the Pb shell. The number of neutrons leaving the Pb shell, satisfying the fission-scintillation coincidence requirement and having more than 550 keV of energy, was estimated by Monte Carlo techniques to be ~1.7 per source neutron. Figure 4 depicts the time response of this subcritical system of shells for neutrons of energy greater than about 550 keV. The upper curve represents the results of a Monte Carlo calculation for the number of neutrons incident on a scintillator per nsec per fission (scaled up by 2.5 to aid in visual comparison with the experimental curve). The lower curve was obtained with the experimental setup used to perform the relative $\bar{\nu}$ measurement. It shows the number of neutrons detected by a proton-recoil scintillator-photomultiplier tube per nsec per fission. Time zero for this curve was chosen arbitrarily. Both curves show a time response of about 60 nsec for decay to 10% of the peak rate.

The decoupling effectiveness of the system shown in Fig. 3 is defined by the relative fraction of prompt fission neutrons from the target nucleus which travel directly to the proton-recoil scintillator detectors or which undergo only elastic scat-

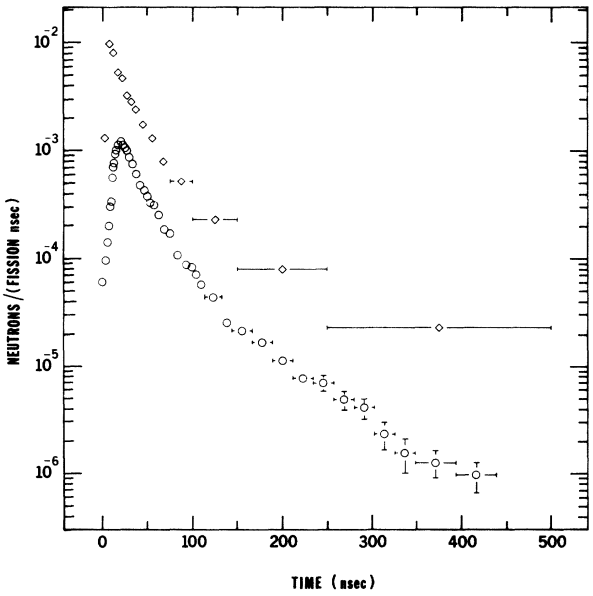

FIG. 4. Time response of neutron multiplicity detector shown in Fig. 3. The lower curve is the actual experimental number of neutrons detected in one of the two scintillators per fission per nsec. The upper curve is the results of a Monte Carlo calculation for the number of neutrons above 0.55 MeV incident on a scintillator per fission per nsec (scaled up by 2.5 to aid in comparing with the experimental curve). Horizontal error bars represent widths of time bins.

tering before entering the scintillators. Monte Carlo calculations indicate that 64% of the detected neutrons come from secondary fissions in the ^{235}U shell. Part of the remaining 36% are prompt fission neutrons which undergo no spectral decoupling whatsoever. Using a ^{252}Cf source in place of the ^{235}U fission chamber of Fig. 3, it was found that about 16% of the detectable prompt fission neutrons travel directly out of the ^{235}U + ^{6}Li + Pb decoupling system with no interactions whatsoever. The rest of the 36% figure is produced by elastic and inelastic scattering processes.

Another estimate for the decoupling effectiveness of the detector shown in Fig. 3 was obtained in the following manner. Using an experimentally determined scintillator response function for the neutron detectors and the Monte Carlo estimate for k, it was calculated that a 10% variation in the Maxwellian temperature of the fission neutrons from the ^{235}U target would produce less than a 2% fictitious variation in $\bar{\nu}$ values.

The neutrons leaving the ^{235}U-^{6}Li-Pb shells were detected in a pair of proton-recoil scintillators. Liquid benzene with solutes similar to those found in NE213[13] was used in these scintillators. It has a pulse-shape-discrimination (PSD) capability which is somewhat better than NE213 as was reported by Czirr.[14] PSD to separate neutron-induced from γ-induced scintillations was achieved by sorting pulses into long (neutron) and short (γ ray) decay times with conventional delay line clipping and zero crossover electronics. Thresholds for each of these detectors were set at about 550-keV proton energy (equivalent to 175-keV γ ray energy). They exhibited an average efficiency of about 50% for fission spectra neutrons above this threshold. This number was obtained experimentally with time-of-flight techniques and a ^{252}Cf fission source. The efficiency in the actual experiment was slightly lower ($\epsilon \sim 45\%$) because the spectrum out of the Pb shell is somewhat lower in average energy than a fission spectrum. This shift is caused by inelastic scattering of fission neutrons off of Pb nuclei.

The fission ionization chamber (see Fig. 3) contained 100 mg of ^{235}U target material (0.4 mg/cm^2) deposited on several 13-μm Al foils which were situated at the center of the ^{235}U-^{6}Li-Pb shells. Fission fragments from the ^{235}U deposited their energy in the 96% A+ 4% CO_2 gas which filled the multiplate ionization chamber to a pressure of ~140 kPa.

The neutron beam was collimated down to an effective area of 6.3 cm^2 at the fission chamber by four pairs of graphite and brass collimators (each ~30 cm long). The defining collimator was recessed about 1 m into the wall to reduce background. The scintillation detectors were shielded from room-background neutrons and γ rays by a lead and borax enclosure. To reduce room background the transmitted neutron beam traversed the remainder of the outer detector cave and 3 m into the earth before leaving the evacuated flight tube.

A block diagram of the electronics used to process both the fission and scintillation signals is shown in Fig. 5. This circuitry produced signals which were used by the data acquisition system to determine which locations on the magnetic drum should be incremented. Signals generated by the circuitry gave the time of flight of the incident neutron which produced the event and identified those events corresponding to prompt neutrons from fission in the target.

The fission signal was derived from the 400-V bias, applied to the multiplate ionization chamber via a coupling capacitor. It was applied to a fast (8-nsec rise time with fission chamber attached) current-sensitive preamplifier. The output of this preamp was routed to a discriminator with bias set just above the α signals which arose from the natural decay of ^{235}U. The fission logic signal from the discriminator was used as a stop pulse in the time digitizer for measurement of the

neutron time-of-flight spectrum. The start pulse was generated when the pulsed electron beam struck the tantalum target (see Fig. 2). The fission logic signal was also used as a 260-nsec time window (signal labeled F in Fig. 5) for detection of coincident events in the proton-recoil scintillators.

The electronics attached to each scintillator-photomultiplier tube detector provided three tag bits for each event within the fission coincidence time window. A parallel set of three tag bits was generated for background events. These two sets of tag bits permitted the simultaneous measurement of the true and random event rates. In addition an analog signal derived from the PSD circuitry was used to insure that the setting of the neutron pulse-shape window did not shift with neutron time of flight. Figure 5 shows only the electronics attached to one of the two scintillators. An identical set was connected to the other detector, and also produced the proper analog signals and tag bits.

Two pulse-height discriminator biases were set on each scintillator-photomultiplier tube event. A pulse-height discriminator (labeled P.H. discr. in the figure) was used to establish the minimum energy for acceptable events. This was set to about 550-keV neutron energy (equivalent to a 175-keV γ ray). The second discriminator (labeled L.E. discr.) was set significantly lower than the pulse-height discriminator—about four times the pulse height corresponding to emission of a single photoelectron from the cathode of the photomultiplier tube. This discriminator provided accurate timing information for the fission coincidence and the PSD circuitry. It also strobed the pileup inspector which was designed to eliminate any event preceded by another event within 3 μsec or followed by one within 0.75 μsec. The output of the PSD circuitry was not used unless a valid event signal was obtained from the pileup inspector. Due to the time necessary for pulse-shape analysis and pileup inspection, the fission signal had to be delayed by at least 1 μsec before performing the fission-scintillator logical coincidence.

Three true-event tag bits were generated for each fission event by a hierarchy of electronic "AND" gates. The first of these was used to signify a coincidence (within the 260-nsec time window produced by the fission logic signal F) between the fission event and a neutron or γ ray event S of sufficient energy to be detected by the proton-recoil scintillator circuitry. The next true tag bit in the series signified that the coincident event, defined by the first tag bit, also satisfied the pile-up inspection requirements thus implying that it

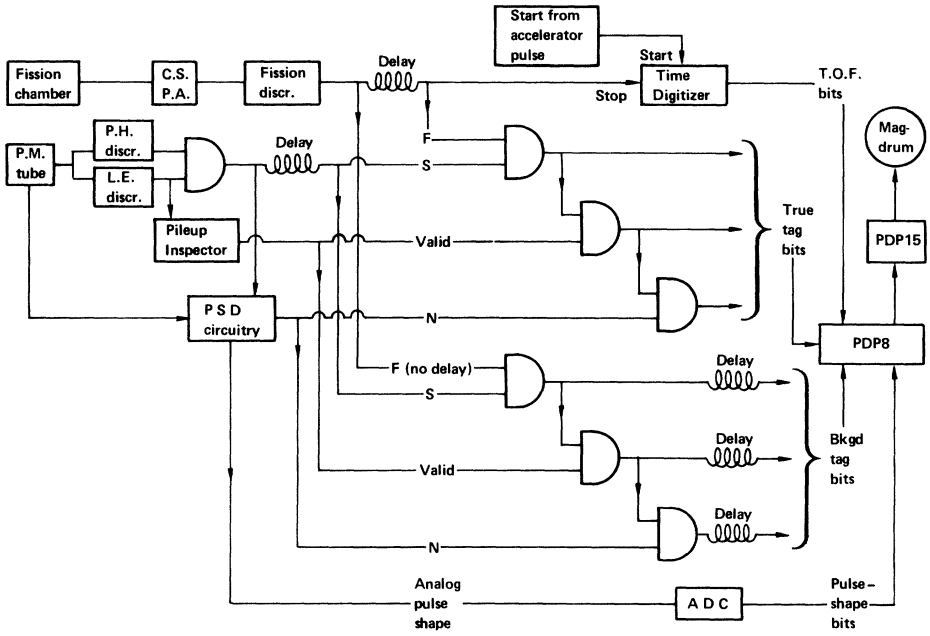

FIG. 5. Electronic circuitry used to process fission and neutron signals. For simplicity only one of the scintillator-photomultiplier tubes is shown. Abbreviations are as follows: C.S.P.A.—current sensitive preamplifier; discr.—discriminator; T.O.F.—time of flight; P.M.—photomultiplier; P.H.—pulse height; L.E.—leading edge; PSD—pulse-shape discrimination; F—fission logic signal; S—scintillator logic signal; N—scintillator neutron logic signal; bkgd—background; Mag-drum—magnetic drum; D—conventional electronic "AND" gate.

was meaningful to check the output of the PSD circuitry. The final tag bit was used to specify that the event which had met the coincidence and pileup requirement had a neutron pulse shape. In this fashion nearly all the dead time induced by pileup was ascertained directly rather than inferred.

The rate of events due to random coincidences between background events in the scintillators and fission chamber events must be obtained to correct the observed event rate for background effects. This background rate was measured by using the fission logic signal F without the delay (see Fig. 5), and a parallel set of logic signals from the scintillator circuitry S, Valid, and N. The background tag bits permit a measurement of the rate of events in which a fission signal has a scintillation signal preceding it by the fission logic delay time. The background correction was then deduced from this asynchronous rate. Binary coded time-of-flight information for each fission event in the energy range of interest along with its associated true-event tag bits, background tag bits, and pulse-shape bits was presented to the data acquisition system.

ANALYSIS

Seven time-of-flight spectra were generated for each proton-recoil detector from the three true-event tag bits and three background tag bits: one for each of the three successive true tag bits, one for each of the three successive background tag bits, and one for no true of background tag bits. For the time-of-flight range corresponding to a particular ^{235}U resonance, $\bar{\nu}$ was then determined (except for small corrections described below) from the total number of fission events accompanied by a neutron in the scintillator divided by the total number of fission events occurring. The number of coincident neutrons was corrected for pileup-induced dead time and background neutrons. The dead-time correction for a particular time of flight involved multiplying the number of coincident neutrons by the ratio of all scintillation events in coincidence with fission events to the number of all those same coincident events which satisfied the pileup inspector. Thus the only assumption involved in the dead-time correction was that coincident neutrons and γ rays are discarded by the pileup inspector with equal probability. This was indeed the case since essentially all pileup was caused by background events. A minor correction for pileup of true events on other true events was made by assuming Poisson statistics for the probability distribution of the number of neutrons in coincidence with a fission event. Similar dead-time corrections were applied to the background neutron information. In this experiment pileups (of background events on true events) induced dead times which ranged from 0.2 to 2% as incident neutron energies increased from 0.5 to 125 eV.

The number of fission-neutron coincidences for a particular time of flight was also corrected for background neutrons. After correcting the measured number of background neutrons for pileup-induced dead time, it was necessary to unfold the asynchronous timing (see experimental section) between fission events and background neutron events. The number of fission events in coincidence with a background neutron in the scintillator occurring at a fixed time before the fission event was measured in the experiment. This number was then multiplied by the ratio of the number of fission events at the time of the background events to the number of fission events occurring after the background events at the fixed asynchronous delay time. The result was then used for the number of background neutrons in coincidence with fission events at each time of flight and was simply subtracted from the number of fission-neutron coincidences to give the number of true fission-neutron coincidences. In the actual experiment the ratio of background to true rates in the neutron detectors ranged from 0.05% to 0.3%.

Each relative $\bar{\nu}$ value presented in this paper represents a sum of data obtained over a given time-of-flight range. No attempt was made to subtract contributions from tails of adjacent resonances underlying the primary resonance. Data accumulated were subdivided into several runs and analyzed separately. Each run for each tube was normalized arbitrarily by dividing all $\bar{\nu}$ numbers by the weighted average $\bar{\nu}$ for incident neutron energies between 0.52 and 114 eV. The final relative $\bar{\nu}$ values reported here represent the weighted average over all these runs.

The errors assigned to each of the $\bar{\nu}$ values presented in this paper represent one standard deviation. They were calculated using the standard method of propagation of errors (based on the total differential) and include only statistical errors. About 97% of the error in each value comes from the error in the number of coincident neutrons (all three true tag bits present).

Values for $\bar{\nu}$ were obtained for a total of 33 isolated resonances in the energy range of this experiment. Twenty-three $\bar{\nu}$ points were also computed for groups of resonances not easily resolved due to their natural widths or experimental broadening from the 1-μsec accelerator neutron pulse width. These 56 $\bar{\nu}$ values are shown in Fig. 6 and Table I. In order to examine gross energy dependent structure, the time-of-flight data were

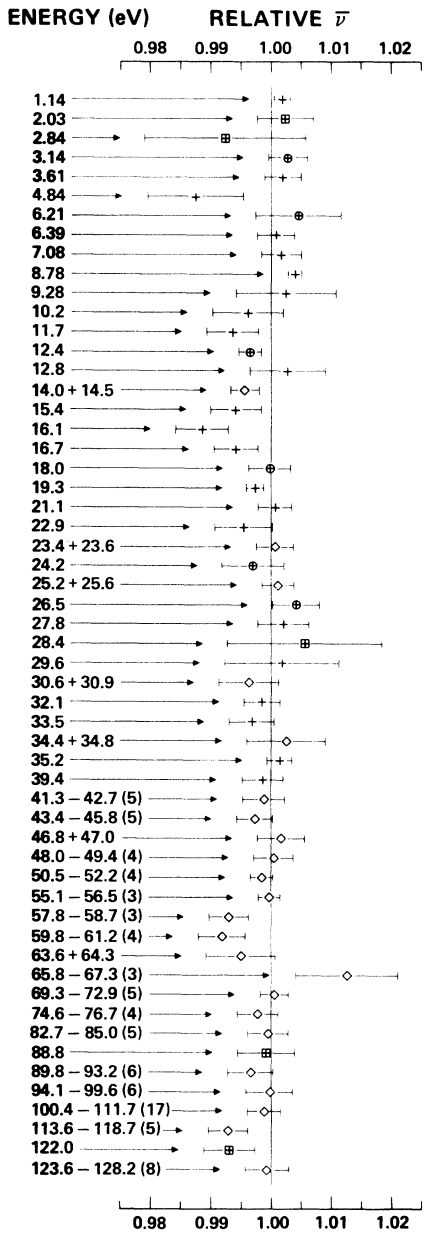

FIG. 6. Relative resonance $\bar{\nu}$ values measured in present experiment. Interpretation of plotted symbols is as follows: The $\oplus$ represents $J=3^-$ resonances; the + represents $J=4^-$ resonances; the $\boxplus$ represents resonances with unassigned spins, and the $\diamond$ represents $\bar{\nu}$ values for groups of resonances. Spins are taken from Ref. 9. Resonance energies are taken from Ref. 10. ( ) indicates the number of unresolved resonances.

grouped into 20 points [see Fig. 7(a)]. Each of these points has a fractional standard deviation of 0.16%. The horizontal error bars shown in Fig. 7(a) represent the energy range used to produce each point. The fission resonances involved in each of these gross feature $\bar{\nu}$ points may be seen by comparing Fig. 7(a) to the raw fission data shown in Fig. 7(b).

DISCUSSION

The results of the present experiment, shown in Fig. 6, evidence a slight amount of structure, although it might be argued that this is within the statistical limits. The purpose of this section is to present facts from the present measurement and previous measurements in support of the hypothesis that there is some real structure in $\bar{\nu}\,(E_n)$ in the resonance region.

The 56 points shown in Fig. 6 give a reduced χ^2 (χ^2/ν) of 1.24—only slightly larger than what would be expected from a random sampling. However, if the calculation is restricted to the 14 points with fractional errors less than 0.3%, the reduced χ^2 is 1.97, implying that perhaps there is some real structure to the data which is being masked by insufficient statistics. In order to examine this possibility further, the resonance structure in the fission data was ignored and the time-of-flight data was grouped into 20 points [see Fig. 7(a) and Table II]. This regrouping makes the hypothesis of structure in $\bar{\nu}\,(E)$ much more plausible. These 20 points have a reduced χ^2 of 3.45—considerably beyond what one would expect for random scatter about a single mean ($\chi^2/\nu = 3.45$ for $\nu = 19$ degrees of freedom is beyond the 0.1 percentage point of the χ^2 distribution).

A recent measurement by Keyworth *et al.*[9] provides information on the resonant spins of many of the data points shown in Fig. 6. Six $J=3^-$ resonances are plotted using the symbol $\oplus$; those 22 with $J=4^-$ are plotted with the symbol +. The weighted mean $\bar{\nu}$ numbers for these two groups of points differ by 0.0010 ± 0.0014, implying no significant spin dependence in $\bar{\nu}$. The error quoted is one standard deviation of the internal error. In addition, two of the stronger resonances, 8.79 and 19.3 eV, have

$$\Delta\bar{\nu} = \bar{\nu}_{8.79} - \bar{\nu}_{19.3} = +0.0067 \pm 0.0018,$$

yet both of these resonances have spin 4^-. Thus it is concluded that the structure in resonant $\bar{\nu}\,(E)$ of $^{235}\mathrm{U}(n,f)$ is uncorrelated with spin.

Recent measurements of resonance $\bar{\nu}$ for the case of ^{239}Pu by Frehaut and Shackelton[11] have demonstrated the presence of some structure in $\bar{\nu}$. This is attributed to enhanced competition between direct fission and the $(n,\gamma f)$ process for the $J=1^+$ states where the fission channel is just beginning to open up. Although ^{235}U fission channels are considerably more open for both initial spin

TABLE I. Resonance $\bar{\nu}$ values (relative to weighted average $\bar{\nu}$ between 0.52 and 114 eV). ( ) indicates the number of unresolved resonances.

Resonance [a] energy (eV)	$\bar{\nu}$	$\sigma_{\bar{\nu}}$	Resonance energy (eV)	$\bar{\nu}$	$\sigma_{\bar{\nu}}$
1.14	1.0018	0.0014	28.4	1.005	0.013
2.03	1.0023	0.0047	29.6	1.0017	0.0095
2.84	0.992	0.013	30.6 +30.9	0.9962	0.0050
3.14	1.0028	0.0032	32.1	0.9984	0.0030
3.61	1.0019	0.0030	33.5	0.9967	0.0037
4.84	0.9874	0.0079	34.4 +34.8	1.0024	0.0065
6.21	1.0045	0.0071	35.2	1.0013	0.0020
6.39	1.0007	0.0031	39.4	0.9985	0.0033
7.08	1.0016	0.0034	41.3 – 42.7(5)	0.9987	0.0035
8.78	1.0039	0.0012	43.4 – 45.8(5)	0.9972	0.0030
9.28	1.0024	0.0083	46.8 +47.0	1.0015	0.0039
10.2	0.9961	0.0059	48.0 – 49.4(4)	1.0003	0.0033
11.7	0.9935	0.0043	50.5 – 52.2(4)	0.9984	0.0019
12.4	0.9964	0.0019	55.1 – 56.5(3)	0.9996	0.0018
12.8	1.0026	0.0063	57.8 – 58.7(3)	0.9930	0.0033
14.0 +14.5	0.9955	0.0023	59.8 – 61.2(4)	0.9918	0.0039
15.4	0.9941	0.0042	63.6 +64.3	0.9950	0.0057
16.1	0.9884	0.0044	65.8 – 67.3(3)	1.0126	0.0085
16.7	0.9941	0.0036	69.3 – 72.9(5)	1.0005	0.0024
18.0	0.9997	0.0035	74.6 – 76.7(4)	0.9978	0.0034
19.3	0.9972	0.0014	82.7 – 85.0(5)	0.9994	0.0034
21.1	1.0005	0.0028	88.8	0.9992	0.0048
22.9	0.9953	0.0048	89.8 – 93.2(6)	0.9966	0.0037
23.4 +23.6	1.0005	0.0031	94.1 – 99.6(6)	0.9997	0.0038
24.2	0.9969	0.0051	100.4 – 111.7(17)	0.9988	0.0028
25.2 +25.6	1.0010	0.0027	113.6 – 118.7(5)	0.9928	0.0033
26.5	1.0040	0.0039	122.0	0.9930	0.0043
27.8	1.0020	0.0043	123.6 – 128.2(8)	0.9993	0.0037

[a] Reference 10.

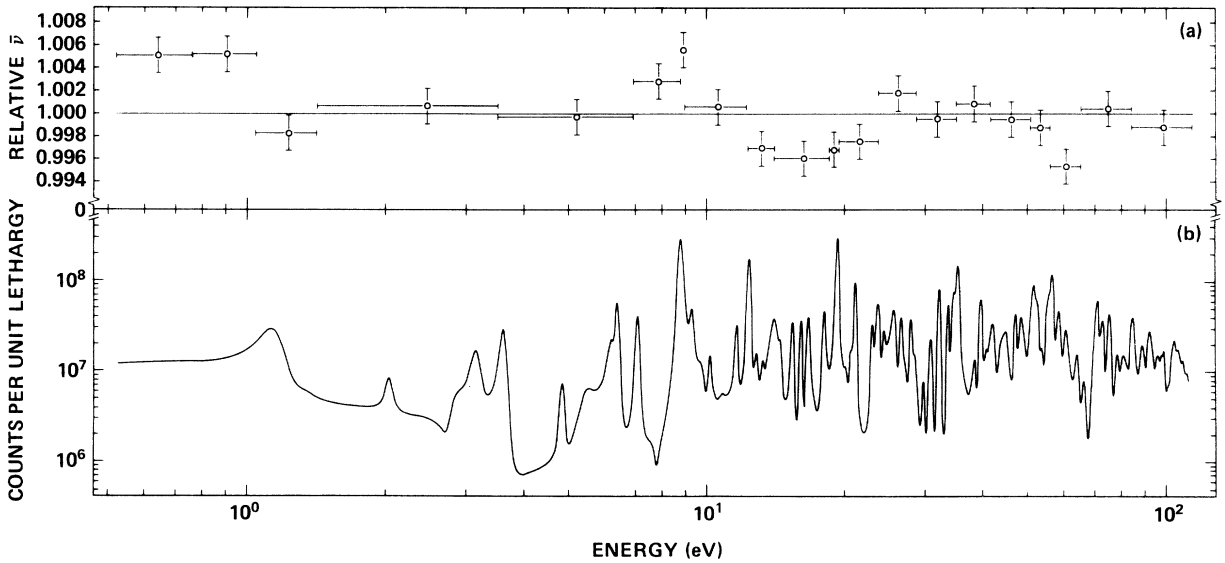

FIG. 7. (a) $\bar{\nu}$ as a function of incident neutron energy, ignoring resonance structure. Horizontal error bars indicate the energy range of summation. The plausibility of structure is enhanced over that in Fig. 6. (b) Raw fission data used to obtain $\bar{\nu}$ (E_n).

TABLE II. Energy averaged $\bar{\nu}$ values (relative to weighted average $\bar{\nu}$ between 0.52 and 114 eV).

Energy range (eV)	$\bar{\nu}$	$\sigma_{\bar{\nu}}$
0.52–0.76	1.0051	0.0016
0.77–1.06	1.0052	0.0016
1.07–1.43	0.9983	0.0016
1.44–3.52	1.0007	0.0016
3.53–6.92	0.9997	0.0016
6.93–8.78	1.0028	0.0016
8.79–9.02	1.0056	0.0016
9.03–12.2	1.0006	0.0016
12.3–14.0	0.9969	0.0016
14.1–18.6	0.9960	0.0016
18.7–19.5	0.9968	0.0016
19.6–23.7	0.9975	0.0016
23.8–28.7	1.0018	0.0016
28.8–35.0	0.9995	0.0016
35.1–41.5	1.0009	0.0016
41.6–50.8	0.9995	0.0016
50.9–56.1	0.9988	0.0016
56.2–65.4	0.9953	0.0016
65.5–84.2	1.0004	0.0016
84.3–114	0.9988	0.0016

states, the statistical accuracy of the present data might warrant an examination of the possible dependence of $\bar{\nu}$ on Γ_f. Figure 8 shows a semilog plot of Γ_f vs $\bar{\nu}$. There is little evidence for any dependence of $\bar{\nu}$ on Γ_f for either spin state, as can be seen from this graph.

The possible correlation of resonance $\bar{\nu}$ with fission-fragment angular or mass asymmetry is a worthwhile area for speculation since all of these parameters should be dependent on the particular fission exit channels that dominate for a given resonance. Using the Pattenden and Postma[15] determination of the coefficient of the second Legendre polynomial $A2$, no evidence was observable for an interdependence of $\bar{\nu}$ and fragment angular asymmetry. A similar comparison of resonance $\bar{\nu}$ with the fission-fragment mass asymmetry data of Cowan, Bayhurst, and Prestwood[6] (see Fig. 9) shows no obvious correlations.

The four parts of Fig. 10 show a comparison of the present results with those of other recent experiments. With the exception of the results of Ryabov *et al.*[2] [Fig. 10(a)], all the sets of $\bar{\nu}$ data show similar patterns (where the statistics are sufficient to facilitate a meaningful comparison). The present experiment [Fig. 10(d)] and that of Reed, Hockenbury, and Block[4] [Fig. 10(b)] quote the smallest errors, thus making a relative comparison more meaningful. The 21 resonances with $\bar{\nu}$ values quoted by both sources give an unweighted

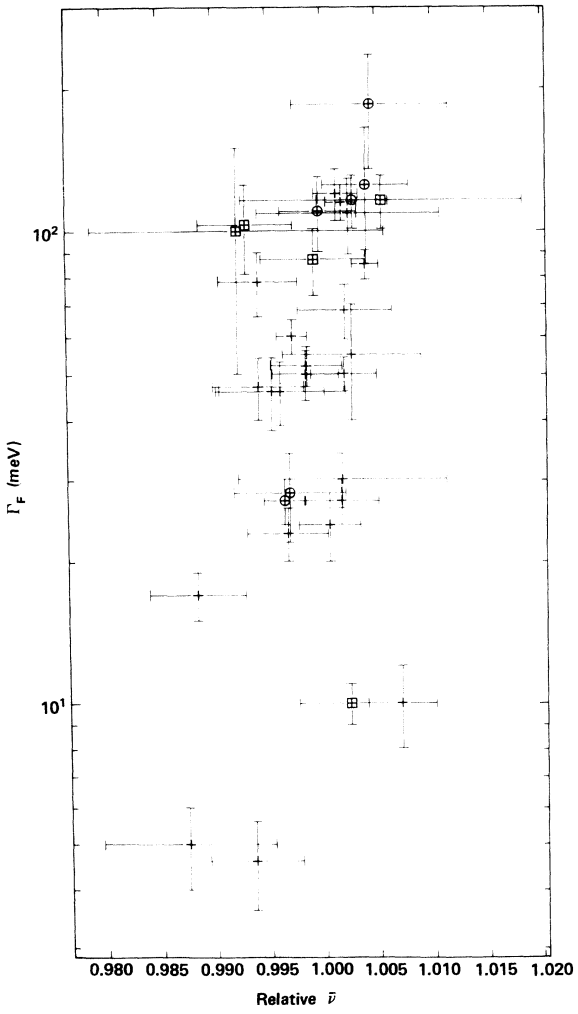

FIG. 8. Relationship between the fission width and relative $\bar{\nu}$. Plot symbols are the same as those defined in Fig. 6. Fission widths are taken from Ref. 10. Note the lack of any apparent correlation.

correlation coefficient

$$\rho = +0.44 \pm 0.22 .$$

This correlation coefficient is statistically significant and provides additional support for the hypothesis that small structure exists in $\bar{\nu}\,(E_n)$. Limiting this comparison to those 10 points which have fractional errors less than 0.4% for both Reed *et al.* data and the present results, the correlation coefficient is $+0.61 \pm 0.16$. Hence, the agreement between relevant portions of the present data and that of Reed *et al.* appears good. Again both experiments imply some small structure in $\bar{\nu}\,(E_n)$. A comparison of 28 resonance $\bar{\nu}$ values common to both the present work and that

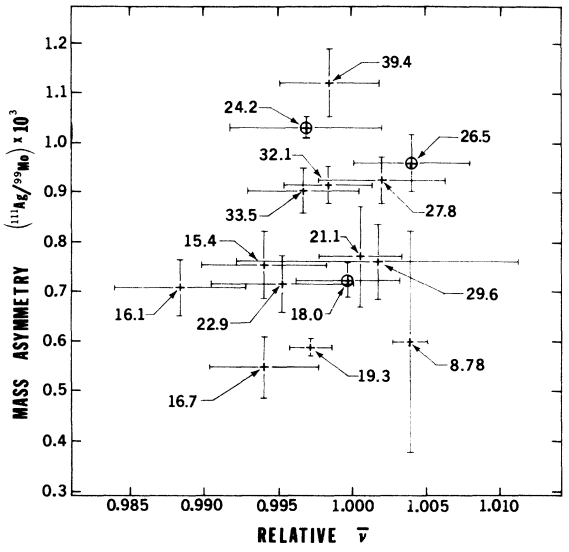

FIG. 9. Relationship between relative $\bar{\nu}$ and fission fragment mass asymmetry. Mass asymmetry information (Ref. 6) has been averaged over two reported data points where necessary to include all of resonance width. Plot symbols and resonance energies are the same as those defined in Fig. 6. Note the lack of any apparent correlation.

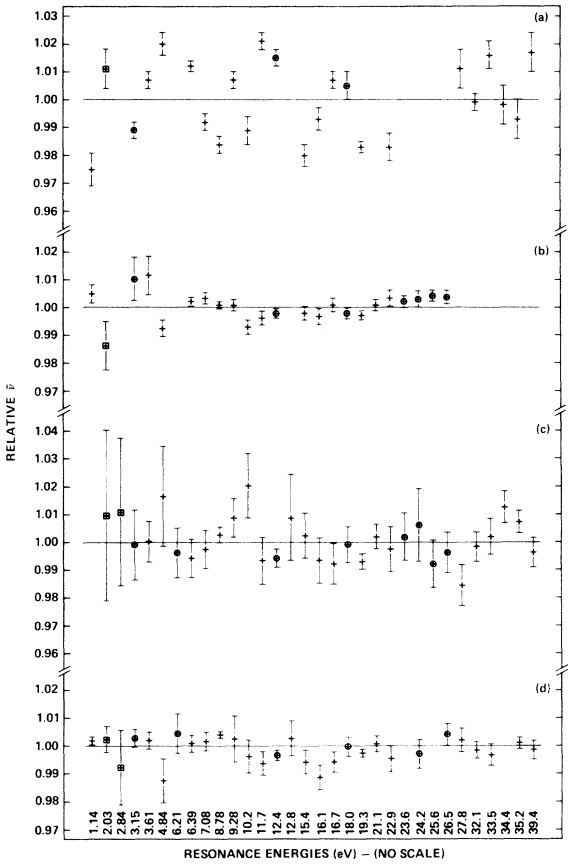

FIG. 10. Comparison of present results with previous measurements. (a) Ryabov *et al.* (Ref. 2). (b) Reed *et al.* (Ref. 4). (c) Frehaut *et al.* (Ref. 11). (d) Portion of present data. Data in (a), (b), and (c) are each individually normalized such that the weighted mean for each group of data is 1. For (d) the normalization of Fig. 6 is used. Symbol notation and resonance energies are the same as those defined in Fig. 6.

of Frehaut *et al.*[11] [Fig. 10(c)] gives $\rho = -0.14 \pm 0.41$. Thus the larger error bars of these data mask any possible correlation. The measurement by Ryabov *et al.*[2] [Fig. 10(a)] shows large variations of $\bar{\nu}$ not observed in this experiment. This disagreement is borne out by a correlation coefficient $\rho = -0.18 \pm 0.19$ on 23 resonance $\bar{\nu}$ data points.

CONCLUSION

The present measurement of resonance $\bar{\nu}$ for neutron-induced fission of ^{235}U shows some small but statistically significant deviations ($\lesssim 0.5\%$) from the mean. In the region of overlap with previous measurements, the present data agree with that of two authors[4,11] but conflict markedly with one other determination.[2] A resonance-by-resonance comparison of these data with initial spin state, fission width, fragment-mass asymmetry, and the angular distribution of fission fragments was made. There appears definitely to be no correlation for ^{235}U between $\bar{\nu}$ and the resonance spin or the fission width. Within the accuracy of this and other experiments measuring mass asymmetry and angular distribution, no evidence of correlation was found with either of these quantities.

ACKNOWLEDGMENTS

The authors would like to thank Dr. J. C. Browne for many helpful discussions, Dr. J. B. Czirr for aid in designing the proton-recoil detectors, Mr. J. Behrens for his method of fission foil preparation, Mr. M. C. Lara for much of the design effort on the ^{235}U spherical shell neutron spectrum decoupler, Mr. R. M. Rodrigues for his help with the electronics design work, and Mr. J. V. McGregor for the necessary mechanical apparatus used in this experiment.

*Work performed under the auspices of the U.S. Energy Research and Development Administration.

[1]S. Weinstein, R. L. Reed, and R. C. Block, in *Proceedings of the Second International Atomic Energy Agency Symposium on Physics and Chemistry of Fission, Vienna, Austria, 1969* (IAEA, Vienna, Austria, 1969), p. 477.

[2]Yu. V. Ryabov, So Don Sik, N. Chikov, and N. Yaneva, Yad. Fiz. 14, 927 (1971) [Sov. J. Nucl. Phys. 14, 519 (1972)].

[3]L. W. Weston and J. H. Todd, in *Proceedings of the Third Conference on Neutron Cross Sections and Technology, Knoxville, Tenn. 1971,* edited by R. Macklin, Report No. CONF-710301 (U.S. AEC Division of Technical Information, Oak Ridge, Tenn., 1971), Vol. 2, p. 861.

[4]R. L. Reed, R. W. Hockenbury, and R. C. Block, Linear Accelerator Project Annual Technical Report No. COO-3058-29, Oct. 1, 1972–Dec. 31, 1972, Rensselaer Polytechnic Institute (unpublished), Vol. 3; R. L. Reed, Ph.D. thesis, Rensselaer Polytechnic Institute, 1969 (unpublished).

[5]J. Terrell, Phys. Rev. 127, 880 (1962).

[6]G. A. Cowan, B. P. Bayhurst, and R. J. Prestwood, Phys. Rev. 130, 2380 (1963).

[7]A. Bohr, in *Proceedings of the United Nations International Conference on the Peaceful Uses of Atomic Energy, Geneva, Switzerland, 1955* (United Nations, New York, 1956), p. 151.

[8]A. Michaudon, *Advances in Nuclear Physics* (Plenum, New York, 1973), Vol. VI, p. 40.

[9]G. A. Keyworth, C. E. Olsen, F. T. Seibel, J. W. T. Dobbs, and N. W. Hill, Phys. Rev. Lett. 31, 1077 (1973).

[10]*Resonance Parameters,* compiled by S. F. Mughabghab and D. I. Garber, Brookhaven National Laboratory Report No. BNL-325 (NTIS, Springfield, Virginia, 1973), 3rd ed., Vol. I

[11]J. Frehaut and D. Shackleton, in *Proceedings of the Third International Atomic Energy Agency Symposium on the Physics and Chemistry of Fission, Rochester, 1973* (IAEA, Vienna, 1973), p. 201.

[12]k is interpreted as the ratio of the number of neutrons in the ith generation to those in the $i-1$th generation for a system involving repeated fissions. A critical (self-sustaining) system is achieved when $k=1$.

[13]Nuclear Enterprises, Ltd., San Carlos, California.

[14]J. B. Czirr, Nucl. Instrum. Methods 88, 321 (1970).

[15]N. J. Pattenden and H. Postma, Nucl. Phys. A167, 225 (1971).